4, the additional 3-O-sulfo group causes—already at the level of the trisaccharide—a stabilization of the skew conformation by about 0.5 kcal mol^{-1}. This stabilization arises from electrostatic interactions, the other energy contributions being unaffected. Caution, however, calls for more refined computations, capable of providing a more comprehensive understanding of the conformational equilibrium.

It is noteworthy that in heparin sequences conversion of one I_{2S} residue from conformation $^1C_4$ to $^2S_0$ can occur through an energy barrier of height similar to that computed for the monosaccharide,[20] without substantially affecting the position of the distant residues. Figure 5 shows molecular models of 4, respectively, for the lowest $^1C_4$ minimum and for the corresponding (i.e., with the closest φ and ψ values) $^2S_0$ minimum. It is apparent that major differences only occur at the iduronate moiety, where the orientation of some substituents drastically changes, while the other parts of the trisaccharide models are almost superimposable: the end-to-end distance (between O(4) of $A^*_{NS,3,6S}$ and O(1) of $A_{NS,6S}$) is 11.85 and 11.76 Å for $^1C_4$ and $^2S_0$, respectively, the mean difference between the atomic coordinates for the end groups being only 0.2 Å. This implies that even the complete conversion from $^1C_4$ to the $^2S_0$ form does not necessarily involve a significant change in the overall shape of the heparin chain.

In conclusion, the present work shows that the conformation of sulfated iduronate residues in heparin can be described in terms of an equilibrium between the $^1C_4$ and $^2S_0$ forms. The relative contribution of these conformers of I_{2S}, and therefore the orientation of its sulfate, carboxylate, and hydroxyl groups, is different in different sequences. This raises the question whether the biological activities associated with binding at the level of these groups are modulated by the unusual conformational flexibility of the iduronate residues. It is interesting in this respect that 3-sulfation, which is crucial for AT-III binding and thus for anticoagulant activity, indeed induces a noticeable change in the conformer equilibrium.

Registry No. 3, 104155-85-3; 4, 104172-26-1; 5, 88096-18-8; 6, 88096-19-9; 7, 92745-16-9; I_{2S}, 69098-37-9; heparin, 9005-49-6.

Structural Analysis of a Glycolipid Head Group with One- and Two-State NMR Pseudoenergy Approaches

J. N. Scarsdale,† R. K. Yu,‡ and J. H. Prestegard*†

Contribution from the Department of Chemistry, Yale University, New Haven, Connecticut 06511, and Department of Neurology, Yale University, School of Medicine, New Haven, Connecticut 06510. *Received March 17, 1986*

Abstract: The solution conformation of the oligosaccharide head group of the glycolipid globoside has been determined with the use of ^1H two-dimensional NMR methods. The intensities of cross peaks in cross relaxation correlated experiments have been analyzed in terms of interproton distances, and the distances have been incorporated as a pseudoenergy in a conformational energy calculation. Minimum energy conformations have been determined by using both one- and two-state models. Conformations are consistent with a previously proposed "L" shape for the molecule. Comparison of the results from the two models suggests the possibility of conformational flexibility to exist for the terminal residue of the head group.

It has long been recognized that NMR cross-relaxation data can provide information on the solution conformation of molecules through the inverse sixth power dependence of intramolecular cross-relaxation rates on internuclear distances. Data in the past have most frequently been obtained through selective irradiation or inversion of a single resonance in a one-dimensional spectrum, followed by the observation of steady state or dynamic Nuclear Overhauser Enhancements (NOEs) on other resonances. More recently, the introduction of two-dimensional analogues of these experiments[1] has improved data acquisition efficiency and resolution to the point where the determination of the solution conformation of biological macromolecules can be attempted. Noteworthy illustrations include applications by Wüthrich and co-workers[2-4] and Kaptein and coworkers[5] to a number of small proteins and polypeptides.

Despite the success of these applications, it is widely recognized that analysis is limited by two assumptions, first that sufficient distance constraints will be observed to permit the unequivocal determination of solution conformation, and second that the observed cross-relaxation rate can be interpreted in terms of a single static conformer rather than a weighted average over all conformers present in solution. Violation of either of these assumptions gives rise to the possibility that the conformer determined to best fit the observed data does not accurately represent the dominant conformer, or in fact any conformer, present in solution.

In this paper we shall explore methodologies which relax these assumptions. We plan to improve structural definition in cases where only limited cross-relaxation data are available through the integration of potential energy calculations with distance constraint

† Department of Chemistry, Yale University.
‡ Department of Neurology, Yale University, School of Medicine.

(1) Jeener, J.; Meier, B. H.; Bachmann, P.; Ernst, R. R. *J. Chem. Phys.* **1979**, *71*, 4546-4553.
(2) Braun, W.; Wider, G.; Lee, K. H.; Wüthrich, K. *J. Mol. Biol.* **1983**, *169*, 921-948.
(3) Havel, T. F.; Wüthrich, K. *J. Mol. Biol.* **1985**, *182*, 281-294.
(4) Williamson, M. P.; Havel, T. F.; Wüthrich, K. *J. Mol. Biol.* **1985**, *182*, 295-315.
(5) Kaptein, R.; Zuiderweg, E. R. P.; Scheek, R. M.; Boelens, R.; van Gunsteren, W. F. *J. Mol. Biol.* **1985**, *182*, 179-182.

0002-7863/86/1508-6778$01.50/0

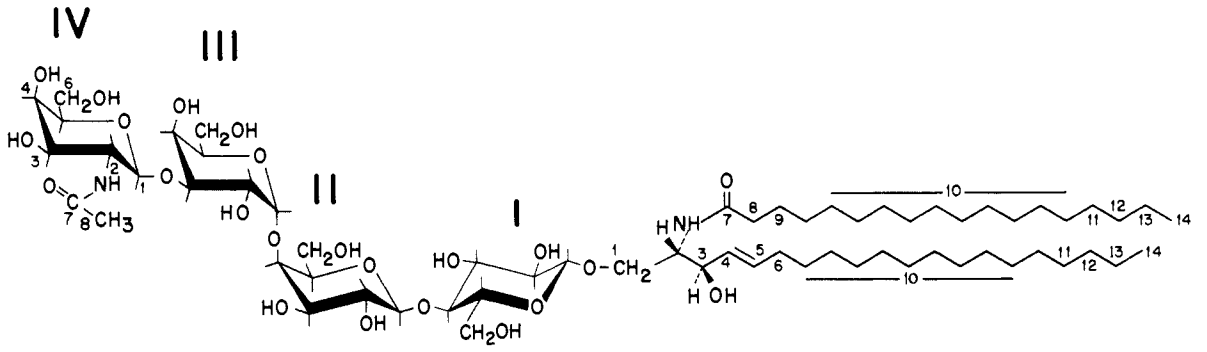

Figure 1. Primary structure of globoside.

data. In these cases, neither potential energy calculations nor cross-relaxation data are sufficient to determine structure alone: the former, because of the neglect of energetic factors, such as solvent interactions, which may be important in determining solution conformation, and the latter, because of multiple conformational solutions where only small numbers of distance constraints are available. In combination, however, an accurate structural definition can arise. Energy calculations can exclude unreasonable NMR conformational solutions, and NMR distance constraints can help select a true conformation from among a set of energetically similar conformers. This approach for integrating potential energy calculations with distance constraint data is similar to the approach used by Kaptein and co-workers in their recent studies on the solution conformation of Lac Repressor headpiece[5] and to that of Clore, et al. on a hexadecapeptide constituting the DNA binding region of the cyclic AMP receptor protein from *Eschericia coli*.[6] However, our approach uses a different pseudoenergy function to integrate NMR data, and we have tailored our approach for a different set of macromolecules, namely cell surface oligosaccharides.

We propose to address the problem of multiple solution conformers by comparing the results of a single state rigid conformational model with those obtained through the use of a two-state conformational model. This model assumes that the observed cross-relaxation rates are the result of a weighted average over discrete conformers present in solution. The methodologies for the integration of potential energy calculations and distance constraint data associated with each of these models shall be discussed in the following sections.

As an illustration of the methodology, we shall attempt the determination of the solution conformation of the oligosaccharide head group of globoside. Globoside is the glycosphingolipid depicted in Figure 1. It has a neutral tetrasaccharide head group and is the major glycospingolipid present in the membrane of human erythrocytes from all but a small minority of individuals. Immunological studies[7,8] have shown that the P-blood group substance is identical with globoside or the globoside oligosaccharide attached to other aglycons. Additional studies[9] have shown that a globoside-like substance present in the membrane of urinary tract epithelial cells serves as a receptor for pathogenic strains of *Escherichia coli* responsible for polynephritis. These determinant and receptor functions make the solution conformation of globoside of considerable interest. The solution conformation of globoside provides a fair test of our methodology in that there are insufficient distance constraints to uniquely determine the solution conformation from cross-relaxation data alone and there has been considerable speculation as to the conformational flexibility of head groups in this and related oligosaccharide cell surface receptors.

Theory

In order to derive interproton distance constraints from two-dimensional NOE cross-peak intensity data (NOESY data), it is first necessary to relate these intensities to cross-relaxation rates. This has been done for a pair of spin one-half nuclei interacting via a through-space dipolar mechanism by Macura and Ernst.[10] In the large molecule limit, cross-peak intensity, a_{kl}, is given as a function of mixing time, τ_m, by

$$a_{kl} = \frac{M_0}{4} \exp(-R_L\tau_m)(1 - \exp(-R_c\tau_m)) \qquad (1)$$

In expression 1 M_0 is the total magnetization present, R_L is a rate constant which represents the rate of magnetication leakage to the lattice, and R_c is twice the negative of the cross-relaxation rate σ_{kl} between the two protons. While this expression is not entirely appropriate for multispin systems, it is a good approximation in the short mixing time limit.[11] Upon substitution of $-2\sigma_{kl}$ for R_c and linearization in the short mixing time limit, expression 1 gives

$$a_{kl} = -\frac{M_0}{2}\sigma_{kl}\tau_m \qquad (2)$$

Thus, for short mixing times, cross-peak intensities in a NOESY experiment are proportional to cross-relaxation rates. Cross-relaxation rates are in turn proportional to the inverse sixth power of internuclear distance. If one considers identical motions to modulate all interactions, the proportionality constants which involve explicit dependence on spectral density functions can be eliminated by considering ratios of cross peaks. This fact, along with expression 2, implies that for sufficiently short mixing times, the correlation between cross peak intensity and internuclear distance is given by

$$r_{ij} = (a_0/a_{ij})^{1/6}r_0 \qquad (3)$$

In expression 3 r_{ij} is the distance to be determined, a_{ij} is the corresponding cross-peak intensity, a_0 is the cross-peak intensity in the same NOESY experiment for a pair of protons at a known fixed distance, and r_0 is that distance. To evaluate r_0 and a_0 it is necessary to find an appropriate proton pair. In naturally occurring glycoconjugates most pyranose rings are believed fixed in a chair conformation,[12,13] so most protons are involved in pairwise interactions with at least one intraring proton at a short known internuclear distance. For example, in β-D-glucosides and β-D-galactosides, the 1–3, 1–5, and 3–5 axial pairs are rigidly fixed at 0.25 nm.[14] In α-D-glucosides and α-D-galactosides, the 1–2 equatorial pair and 3–5 axial pairs are rigidly fixed at 0.25 nm.[15]

(6) Clore, G. M.; Gronenborn, A. M.; Brünger, A. T.; Karplus, M. *J. Mol. Biol.* **1985**, *186*, 435–455.
(7) Marcus, D. M.; Naiki, M. A.; Kundu, S. K. *Proc. Natl. Acad. Sci. U.S.A.* **1976**, *73*, 3263–3267.
(8) Marcus, D. M.; Kundu, S. K.; Suzuki, A. *Semin. Hematol.* **1981**, *18*, 63–71.
(9) Källenius, G.; Svensson, S. B.; Möllby, R.; Cedergren, B.; Hultberg, H.; Windberg, J. *Lancet* **1981**, *2*, 604–606.
(10) Macura, S.; Ernst, R. R. *Mol. Phys.* **1980**, *41*, 95–117.
(11) Kumar, A.; Wagner, G.; Ernst, R. R.; Wüthrich, K. *J. Am. Chem. Soc.* **1981**, *103*, 3654–3658.
(12) Altona, C.; Haasnoot, C. A. G. *Org. Magn. Reson.* **1980**, *13*, 417–429.
(13) Durette, P. L.; Horton, D. *Adv. Carbohyd. Biochem.* **1971**, *26*, 49–125.
(14) Longchambon, F.; Ohannessian, D. A.; Neuman, A. *Acta Crystallogr.* **1975**, *B31*, 2623–2627.

It is not always possible to satisfy the short mixing time assumption while maintaining an adequate signal-to-noise ratio. For this reason we also consider the possibility of fitting two-dimensional data to an equation valid for longer τ_m values, and we consider the possibility of using one-dimensional data. For two-dimensional data on a pair of spins, the ratio of cross-peak intensity to auto-peak intensity for any value of τ_m is given by

$$\frac{a_{kl}(\tau_m)}{a_{kk}(\tau_m)} = \frac{1 - e^{(-R_c\tau_m)}}{1 + e^{(-R_c\tau_m)}} \quad (4)$$

R_c can be extracted by fitting data at any number of τ_m mixing times to this equation. For one-dimensional NOE measurements, obtained by selective irradiation, the time dependence of the enhancement, η_{ij}, in the limit of simple dipolar interaction of a pair of spins, is given as a function of irradiation time by[16]

$$\eta_{ij} = (\sigma_{ij}/\rho)(1 - \exp(-\rho t)) \quad (5)$$

In expression 5, σ_{ij}, as before, represents the cross-relaxation rate between nuclei i and j, ρ represents the overall relaxation rate for the nucleus being irradiated, and t is the time of irradiation. Values of σ_{ij} or R_c obtained from either of the above expressions can be converted to distance constraints with suitable reference measurements. In order to integrate the distance constraint data, obtained from two-dimensional cross-relaxation data with potential energy calculations, we have chosen to treat the distance constraints as a pseudoenergy. The energy for any given conformer is defined as the sum of the pseudoenergy and the contribution from the potential energy calculation. By treating the constraints in such a manner we are able to determine by an energy minimization procedure a preferred geometry for the molecule under consideration. While we could have used any of a number of energy calculation programs, we have chosen to use Bock and Lemieux's Hard Sphere Exo-Anomeric (HSEA) program, obtained from the depository for unpublished data of the National Research Council of Canada. This program has predicted conformations of the oligosaccharide moieties of glycolipids and glycoproteins, which are in a number of instances consistent with NMR data and with crystallographic data on model oligosaccharides.[17-19]

The term we have added to reflect the distance constraints is given by

$$E_{ab} = W[\mathrm{ABS}(r_{ab}^{-6} - r_{0ab}^{-6}) - r_{0ab}^{-6}] \quad (6)$$

In expression 6 r_{0ab} is the distance between two protons determined on the basis of NOE measurements, r_{ab} is the distance between two protons at any stage in the calculation, and W is a weighting factor. Such a function has a minimum at $r_{ab} = r_{0ab}$ with the depth of the minimum proportional to r_{0ab}^{-6}. Energies become more positive to either side of the minimum with a r_{ab}^{-6} dependence. Thus, energies correctly mimic the precision of the NOE data at various distances.

In our calculations, an attempt is made to add this energy term for all interproton distances between different residues regardless of whether or not an NOE is observed. In cases where an enhancement is observed between two resonances, r_0 is set equal to the distance derived from NMR data. In cases where no enhancement is observed, r_0 is set equal to some threshold beyond which no enhancement above the signal-to-noise level is expected, in our case 0.4 nm. At this distance energy contributions are very small and the inclusion of the energy term merely excludes conformers in which the corresponding internuclear distances would be too short.

In the above discussion, we explicitly assume a single rigid conformer to represent the molecular geometry. In certain cases, it is possible to relax this assumption. If two or more conformers were to exist and interconvert on a time scale short compared to the cross-relaxation time, but long compared to correlation times important for spin relaxation ($10^{-8} < \tau < 10^{-2}$), the observed cross-relaxation rate can be represented as the average of cross-relaxation rates for each conformer. If we also assume that the relative energies of the various conformers are approximated by the potential energy calculation in the absence of constraints, we can model the behavior without the introduction of additional variables. The average cross-relaxation rate σ_{ab} is then given by

$$\sigma_{ab} = \frac{e^{(-E_1/kT)}\sigma_{1ab} + e^{(-E_2/kT)}\sigma_{2ab}}{e^{(-E_1/kT)} + e^{(-E_2/kT)}} \quad (7)$$

In expression 7 E_1 and E_2 are the energies of the model conformers, taken from potential energy calculations alone, σ_{1ab} and σ_{2ab} are the cross-relaxation rates between a given pair of protons in the model conformers, k is the Boltzmann constant, and T is the temperature at which the cross-relaxation data were obtained. The pseudoenergy contribution in terms of intramolecular cross-relaxation rates may then be written as

$$E = (W/C)[\mathrm{ABS}(\sigma_{ab} - \sigma_{0ab}) - \sigma_{0ab}] \quad (8)$$

where σ_{0ab} represents the cross-relaxation rate between two protons determined on the basis of the initial rate from the NOE data, C represents a constant of proportionality which relates the inverse sixth power of internuclear distance to an observed cross-relaxation rate, W represents a weighting factor, and σ_{ab} is the calculated average cross-relaxation rate for a given pair of conformers. The overall energies for the two-state calculation are defined as the weighted sum of the contributions of HSEA energies from each conformer plus the distance constraint pseudoenergies. The two-state model was implemented by treating the two conformers as a pair of noninteracting molecules with the geometries of each molecule being varied independently to permit a full search of conformational space for each of the two conformers.

Although eq 7 and 8 may be easily extended to any multiple state model, we shall apply them only in the two-state limit. in the event that the two-state model gives rise to a significant improvement in fitting the experimental data, the result must be interpreted with considerable caution. There are, of course, three- and four-state models, as well as models based on a more rapid sampling of conformational space, which we have not considered. Since we have not considered these alternate models, and because of the inherent assumptions concerning the relative energies of the various conformers, it may be best to take an improvement in fit of the two-state over the one-state model as evidence that the single-state model is inadequate to explain the observed data and that some form of conformational averaging is important.

Experimental Section

Globoside (2 mg) obtained from human erythrocytes and kindly provided by Dr. S. Ando of the Tokyo Metropolitan Institute of Gerontology was prepared for high-resolution NMR analysis as described previously.[20] This sample was dissolved in 0.4 mL of Me_2SO-d_6-D_2O (98:2 (v/v)). Deuterated solvents were obtained from Merck and Co., St. Louis, MO, or Aldrich Inc., Milwaukee, WI.

All spectra were acquired on a Bruker WM-500 equipped with an Aspect 2000A computer and employing quadrature detection. One-dimensional spectra were obtained at 323 K with 256 transients, 4K complex points, a sweep width of 3205 Hz, and a 1.2-s recycling rate.

Two-dimensional pure absorption NOE spectra were obtained at 303 K with the pulse sequence and phase cycling of States et al.[21] In order to achieve quadrature in the F_1 dimension 192 real and 192 imaginary t_1 points were acquired and stored separately. Each t_1 point consisted of 1K complex points over a 3205-Hz sweep width averaged for 64 transients with a 1.2-s repetition rate. Data sets were obtained for mixing times of 250 and 500 ms. All two-dimensional data sets were processed

(15) Sheldrick, B. *Acta Crystallogr.* **1976**, *B32*, 1016-1020.
(16) Dobson, C. M.; Olejniczak, E. T.; Poulsen, F. M.; Ratcliffe, R. G. *J. Magn. Reson.* **1982**, *48*, 97-110.
(17) Lemieux, R. U.; Bock, K.; Delbaere, L. T. J.; Koto, S.; Rao, V. S. *Can. J. Chem.* **1980**, *58*, 631-653.
(18) Bock, K.; Arnarp, J.; Lönngren, J. *Eur. J. Biochem.* **1982**, *129*, 171-178.
(19) Sabesan, S.; Bock, K.; Lemieux, R. U. *Can. J. Chem.* **1984**, *62*, 1034-1045.
(20) Koerner, T. A. W., Jr.; Prestegard, J. H.; Demou, P. C.; Yu, R. K. *Biochemistry* **1983**, *22*, 2676-2687.
(21) States, D. J.; Haberkorn, R. A.; Reuben, D. J. *J. Magn. Reson.* **1982**, *48*, 286-292.

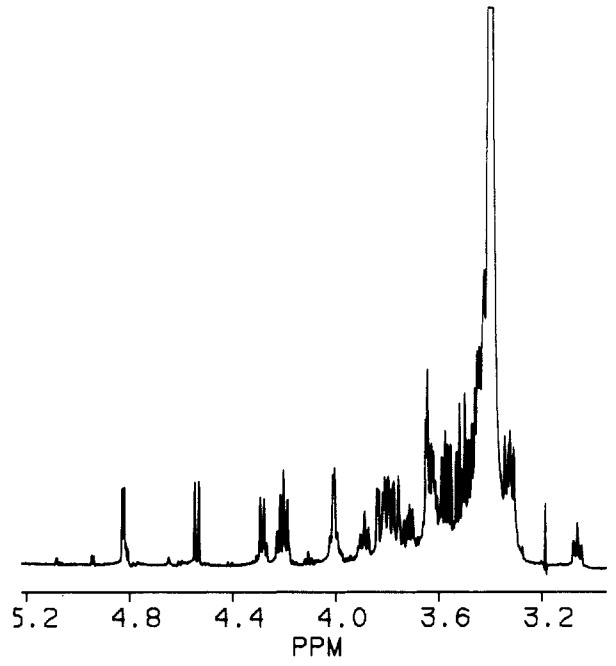

Figure 2. Plot of the anomeric and the ring proton region of the one-dimensional spectrum of globoside obtained with the experimental parameters mentioned in the text. All chemical shifts are referenced to the α-galactose anomeric proton at 4.83 ppm, which is the value given in.[23]

Table I. Chemical Shifts for Globoside in Me_2SO-d_6·D_2O at 323 K

residue	1	2	3	4	5	6a	6b
IV (βGalNAc)	4.54	3.77	3.46	3.67	3.42	3.60	3.57
III (αGal)	4.82	3.82	3.65	4.00	4.15	3.49	
II (βGal)	4.24	3.33	3.43	3.84	3.58	3.65	3.77
I (βGlc)	4.14	3.08	3.34	3.29	3.29	3.63	3.76

with an FTNMR program written by Dr. D. R. Hare running on a VAX 11/750 computer. Data were processed with cosine bell weighting functions in both dimensions and zero filling in the t_1 dimension to yield a 1K by 1K data matrix.

In order to obtain cross-peak intensities from two-dimensional data it is necessary to use cross-peak volumes. These volumes were obtained with a two-dimensional trapezoidal rule approximation. Only the volume above a base plane at the average level of a rectangular region surrounding the cross peak was considered. The use of a base plane offers the advantage that it serves to remove bias introduced into cross-peak volumes by changes in the base-line level. Volumes were computed for several different choices of base planes in order to obtain error limits on cross-peak volumes. For a cross peak between protons at 0.3 nm separation, volume errors were typically 20%. An average error over all cross peaks, along with standard error propagation methods, was used to estimate errors in the various distance constraints.

For comparison purposes, several one-dimensional NOE experiments were also conducted. These were conducted at 303 K with difference spectroscopy.[22] Spectra were obtained with a 3205-Hz sweep width and a 4.2-s repetition rate, 4K complex points, and a total of 256 transients. Experiments were obtained for irradiation times of 500, 750, 1000, and 1250 ms in order to investigate more completely the time course of magnetization transfer.

Results

Figure 2 shows a one-dimensional spectrum of globoside dissolved in Me_2SO-d_6·D_2O. This spectrum was in large part assigned in a previous study.[23] Additional assignments were made through the use of a coupling correlated spectroscopy (COSY) experiment having resolution somewhat better than the spectrum used for the initial assignments. A complete list of resonance assignments is presented in Table I. We will focus our attention on the anomeric resonances between 4.1 and 4.9 ppm. There are four such resonances, each corresponding to one of the four sugar rings in globoside. The resonance at 4.82 ppm with the small coupling constant is clearly the anomeric proton of the α-D-galactose. The others at 4.54, 4.24, and 4.14 ppm correspond to the β-D-GalNAc residue, the β-D-galactose residue, and the β-D-glucose residues, respectively.

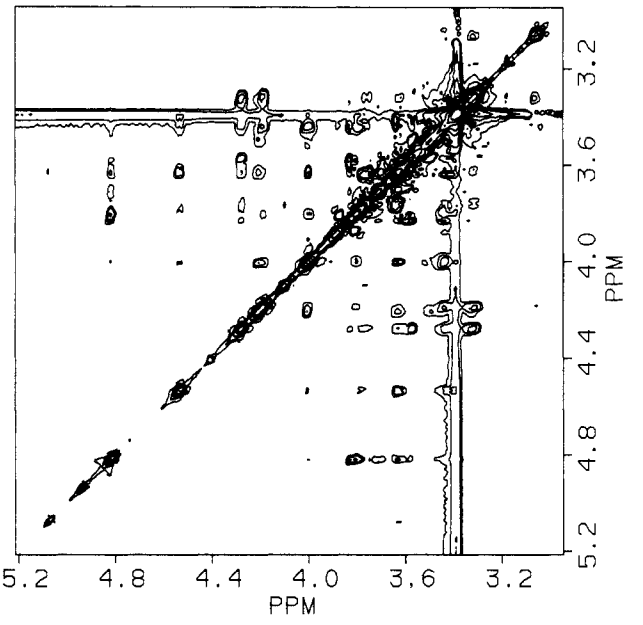

Figure 3. Contour plot of the same region of NOESY experiment obtained with 250 ms mixing time. All constraints used in calculation were taken from this region of this data set.

Figure 3 presents a contour plot of a pure absorption NOESY experiment obtained with a mixing time of 250 ms. In such an experiment there are two classes of cross peaks connecting anomeric resonances to other resonances in the spectrum: those due to interactions with protons on the same residue and those due to interactions with protons on adjacent residues. In each case intensities are proportional to the inverse sixth power of the distance of the proton from the anomeric proton. Given the signal-to-noise ratio in these experiments, only peaks for protons within 0.35 nm are observed. For β-D-glucosides and β-D-galactosides, one expects to see 1–3 and 1–5 axial intraresidue connectivities at 0.25 nm. For α-D-glucosides and α-D-galactosides, one expects to see only a 1–2 equatorial intraring connectivity. Given the previous assignments these are easily found. For example, in the column through the β-galactose anomeric resonance at 4.24 ppm, a cross peak at 3.43 ppm is to the 3 proton, and a cross peak at 3.58 ppm is to the 5 proton of the same residue. These cross peaks can be integrated to provide distance standards for the determination of distances between interresidue proton pairs.

Examination of Figure 3 shows one or more additional cross peaks for each anomeric resonance which must correspond to interresidue cross peaks. The strongest interresidue peaks are in fact assigned to anomeric-transglycosidic proton connectivities. For example, in the case of the β-galactose residue the interresidue peak at 3.29 ppm corresponds to the 4 proton of glucose. Intensities of these cross peaks can obviously be interpreted in terms of *trans*-glycosidic distances. These distances are clearly a function of the torsional angles ϕ and ψ which define the geometry of a glycosidic linkage. ϕ is the torsional angle defined by the anomeric proton, anomeric carbon, glycosidic oxygen, and glycosidic carbon, and ψ is the dihedral angle defined by the anomeric carbon, glycosidic oxygen, glycosidic carbon, and glycosidic proton. Clockwise rotations viewed from the anomeric end are considered positive. Examination of the energetics of the glycosidic linkage for a wide variety of compounds has shown certain preferred angular ranges ($\phi = \pm 60 \pm 15$), ($\psi = 0 \pm 30$).[24] In this range,

(22) Richarz, R.; Wüthrich, K. *J. Magn. Reson.* **1978**, *30*, 147–150.
(23) Koerner, T. A. W., Jr.; Scarsdale, J. N.; Prestegard, J. H.; Yu, R. K. *J. Carbohydr. Chem.* **1984**, *3*, 565–580.
(24) Thørgeson, H.; Lemieux, R. U.; Bock, K.; Meyer, B. *Can. J. Chem.* **1982**, *60*, 44–57.

Table II. Distance Constraint Data for Globoside, Dissolved in Me_2SO-d_6·D_2O

	r(250)[a]	r(2-spin)[b]	r(1-dimensional)[c]
IV(1)–III(3)	0.23 ± 0.003	0.23	0.25
IV(1)–III(4)	0.29 ± 0.009	0.31	0.28
IV(1)–IV(3)	0.25[d]	0.25[d]	0.25[d]
IV(1)–IV(5)	0.25[d]	0.25[d]	0.25[d]
III(1)–II(4)	0.24 ± 0.003	0.22	0.25
III(1)–II(5)	0.35 ± 0.02	0.32	0.32
III(1)–II(6a)	0.26 ± 0.004	0.28	0.30
III(1)–II(6b)	0.26 ± 0.004	0.28	
III(1)–III(2)	0.25[d]	0.25[d]	0.25[d]
III(5)–III(3)	0.25[d]	0.25[d]	
II(1)–I(4)	0.21 ± 0.002	0.21	
II(1)–I(6a)	0.28 ± 0.005	0.28	
II(1)–I(6b)	0.26 ± 0.003	0.30	
II(1)–II(5)	0.25[d]	0.25[d]	

[a] Distances obtained by using expression 3 for cross-peak intensity data from NOESY experiment obtained with mixing time of 250 ms. [b] Distances obtained by using expression 4 to fit cross-peak intensity data for NOESY experiments obtained with both 250 and 500 ms mixing times. [c] Distances obtained by using expression 5 to fit buildup of NOE in one-dimensional experiments, obtained through selective irradiation of a given anomeric resonance. [d] Rigidly fixed proton pair used as a standard in computing interresidue distances.

the *trans*-glycosidic proton distance is within 0.25 nm or less and should give strong cross peaks. Integration and quantitation of these primary interresidue cross peaks can improve conformational definition.

Additional weaker cross peaks are observed for all anomeric resonances. For example, for the β-galactose anomeric resonance, one sees connectivities to the 6a and 6b protons of glucose at 3.63 and 3.76 ppm, respectively. These weaker cross peaks provide additional distance constraints and are particularly useful in testing one- vs. two-state models.

Distance constraints and their associated errors were derived through the use of expression 3 with only the 250-ms data. Results are summarized in Table II. In order to test the validity of the short mixing time assumption used in expression 3, we have chosen to compare the 250-ms constraints with constraints from the ratios of cross-relaxation rates obtained through analyzing the time dependence of cross-peak intensities using eq 4 and data from both the 250- and 500-ms sets. The distance constraints obtained from such a fit are presented in Table II. In general it is noted that the constraints are in excellent agreement with those obtained through the use of expression 3.

We have also chosen to compare constraints determined with eq 3 with constraints obtained from the analysis of time-dependent one-dimensional NOE measurements using eq 5. The distance constraints obtained from one-dimensional data on residues III and IV of globoside by irradiating the anomeric proton resonance are presented in Table II. For both residues, the constraints obtained by fitting one-dimensional NOE data agree quite well with those determined on the basis of two-dimensional data.

In order to convert the constraints listed in Table II into conformational data, they were converted to pseudoenergies and incorporated in an energy calculation program, as described in the Theory section. Additional constraints were added in cases where no enhancement was observed by assigning a value of 0.4 nm to the corresponding distance. For each adjacent pair of residues, calculations were carried out for three different weightings of the distance constraint pseudoenergies relative to the HSEA energies. In the first weighting scheme, the pseudoenergy at $r_0 = 0.3$ nm was 2.8 kcal/mol, which corresponds to allowing the HSEA energies to dominate. In the second weighting scheme, the pseudoenergy at $r_0 = 0.3$ nm was 11.2 kcal/mol which corresponds to allowing the HSEA energies and the distance constraint pseudoenergies to have comparable influence in determining conformation. In the final scheme, the pseudoenergy at $r_0 = 0.3$ nm was 44.8 kcal/mol which corresponds to allowing distance constraint pseudoenergies to dominate.

The HSEA program functions via a grid research mechanism in which the internal geometry of each residue is assumed fixed. In the calculations, crystal structure data were used for each residue.[19,25] The use of crystal structures for the residue conformations is in most cases valid because of the dominance of a single chair form for the sugars in globoside.[12,13] However, some concern must be expressed in cases where cross peaks to methylene protons of an exocyclic CH_2OH group are used to derive distance constraints because these groups do not always adopt the same rotational state in solution as is observed in the crystal. In the case of the CH_2OH group of β-glucose, the coupling patterns between the H5 and H6b resonances and the presence of cross peaks between the H5 and H6b resonances and the H4 and H6a resonances are consistent with the orientation of the CH_2OH group in the crystal structure. In this case the crystal structure orientation of the CH_2OH group was used and constraints to the I(6a) and I(6b) protons were assigned the same weight as other distance constraints. In the case of the exocyclic CH_2OH groups for the other residues it was not possible to determine whether the coupling constant and the NOE data were consistent with the orientation of the CH_2OH groups in the crystal structures. In each of these cases the orientations of the CH_2OH groups from the crystal structures were used, but the constraints involving protons on these groups were assigned half the weight of other constraints.

The molecule was built stepwise starting from the GalNac terminal end. At each addition only the ϕ,ψ pair of the newly added residue was allowed to vary, with the geometry of existing residues fixed by previously determined energy minima. This stepwise procedure for determining conformation ignores to some extent the possibility of long-range residue interactions. However, allowing all angles to vary simultaneously was computationally prohibitive. A limited exploration of energetics starting from the ceramide end did, however, indicate only a minimal effect on final conformations. Conformational data for each of the four residues in globoside obtained by using each of the three weightings from the one- and two-state models are presented in Table III.

In order to compare the one- and two-state models and assess deviation from agreement with NMR data at each pseudoenergy weighting, the sum of the squares of the deviations between the calculated and observed cross-relaxation rates were calculated and scaled by the square of the deviation of a single measurement. These deviations are reported in Table III as χ^2 values. According to the χ^2 test the ratio of these sums to the variance in a single measurement should approach but not fall below the number of independent measurements when an adequate model for the behavior is employed. The number of independent measurements is given at the head of the section for each pair of residues.

Some additional understanding of the deviations can be obtained by direct comparison of the calculated and measured cross-relaxation rates. These are presented in Table IV. Largest deviations occur in cases where cross relaxation to an exocyclic methylene is involved. Some of this may arise because of our inability to precisely define a rotational state for these groups. In cases where cross peaks are observed to geminal methylene protons, Kay et al.[26] have also shown that a simple first-order analysis of relaxation data may not be entirely adequate for extracting distance constraints. Aside from these deviations agreement approaches experimental error for most models.

Discussion

It is clear from the conformational data in Table III that the minimum energy conformer determined from the HSEA energies alone (weighting 0) and from the combination of HSEA energies and distance constraint pseudoenergies are different. As NMR pseudoenergies are weighted more heavily, both the Gal(β1–4)Glc (II–I) and GalNac(β1–3)Gal (IV–III) linkages show moderate departures from the corresponding HSEA minima with ϕ,ψ angles for the II–I linkage moving from $\phi = 60$, $\psi = -10$ to $\phi = 20$, $\psi = 0$ and ϕ,ψ angles for the IV–III linkage moving from $\phi = 60$,

(25) Takagi, S.; Jeffery, G. A. *Acta Crystallogr.* **1979**, *B35*, 902–906.
(26) Kay, L. E.; Holak, T. A.; Johnson, B. A.; Armitage, I. M.; Prestegard, J. H. *J. Am. Chem. Soc.* **1986**, *108*, 4242–4244.

Table III. Conformational Data for Globoside Dissolved in Me_2SO-d_6·D_2O

pseudoenergy scaling factor	glycosidic dihedral angles, 1-state model	$\chi^2$1s[c]	glycosidic dihedral angles, 2-state model	fractional population	$\chi^2$2s[c]
III, IV		56[b]			56[b]
0	$\phi = 60, \psi = -10$	113			
2.8[a]	$\phi = 40, \psi = -50$	60	$\phi = 40, \psi = -50$[d]	0.83	54
			$\phi = 40, \psi = -70$[e]	0.17	
11.2[a]	$\phi = 40, \psi = -50$	60	$\phi = 20, \psi = -40$[d]	0.65	47
			$\phi = 80, \psi = 20$[e]	0.35	
44.8[a]	$\phi = 40, \psi = -50$	60	$\phi = 0, \psi = 30$[d]	0.53	46
			$\phi = 100, \psi = -20$[e]	0.47	
II, III		95[b]			95[b]
0	$\phi = -40, \psi = -10$	201			201
2.8[a]	$\phi = -50, \psi = -10$	123	$\phi = -50, \psi = -10$[d]	0.81	127
			$\phi = 20, \psi = 30$[e]	0.19	
11.2[a]	$\phi = -50, \psi = -10$	123	$\phi = -50, \psi = -10$[d]	0.81	127
			$\phi = 20, \psi = 30$[e]	0.19	
44.8[a]	$\phi = -50, \psi = -10$	123	$\phi = -50, \psi = -10$[d]	0.81	127
			$\phi = 20, \psi = 30$[e]	0.19	
I, II		154[b]			154[b]
0	$\phi = 60, \psi = -10$	1871			
2.8[a]	$\phi = 20, \psi = 0$	409	$\phi = 20, \psi = -10$[d]	0.85	400
			$\phi = 20, \psi = 0$[e]	0.15	
11.2[a]	$\phi = 20, \psi = 0$	409	$\phi = 20, \psi = -10$[d]	0.85	400
			$\phi = 20, \psi = 0$	0.15	
44.8[a]	$\phi = 20, \psi = 0$	409	$\phi = 20, \psi = -10$[d]	0.85	400
			$\phi = 20, \psi = 0$[e]	0.15	

[a] Depth of minimum in kcal/mol for $r_0 = 0.3$ nm. [b] Number of independent measurements. [c] Calculated using relationship $\chi^2 = \sum(\sigma_{ij} - \sigma_{ij0})^2/\Delta\sigma^2$. [d] ϕ, ψ angles for conformer 1. [e] ϕ, ψ angles for conformer 2.

Table IV. Comparison of Cross-Relaxation Rates for the Various Models

		one-state				two-state		
	exptl[a]	0[b]	2.8[b]	11.2[b]	44.8[b]	2.8[b]	11.2[b]	44.8[b]
IV(1)-III(3)	−2.46 ± 0.14	−1.90	−2.46	−2.46	−2.46	−2.12	−2.24	−2.16
IV(1)-III(4)	−0.58 ± 0.08	−0.10	−0.58	−0.58	−0.58	−0.60	−0.56	−0.44
IV(4)-III(6a)[c]	≤−0.10	−0.10	−0.38	−0.38	−0.38	−0.36	−0.10	−0.06
III(1)-II(4)	−2.18 ± 0.12	−3.04	−2.38	−2.38	−2.38	−2.56	−2.56	−2.56
III(1)-II(5)	−0.24 ± 0.10	−0.10	−0.10	−0.10	−0.10	−0.10	−0.10	−0.10
III(1)-II(6a)	−1.22 ± 0.10	−1.32	−1.36	−1.36	−1.36	−1.14	−1.14	−1.14
III(1)-II(6b)	−1.34 ± 0.12	−1.34	−1.64	−1.64	−1.64	−1.36	−1.36	−1.36
III(5)-II(4)[c]	≤−0.10	−0.40	−0.38	−0.38	−0.38	−0.32	−0.32	−0.32
II(1)-I(4)	−5.76 ± 0.24	−2.10	−5.48	−5.48	−5.48	−2.94	−2.94	−2.94
II(1)-I(6a)	−1.70 ± 0.12	−0.42	−0.36	−0.36	−0.36	−0.40	−0.40	−0.40
II(1)-I(6b)	−1.08 ± 0.12	−1.70	−0.78	−0.78	−0.78	−0.88	−0.88	−0.88

[a] Obtained by using eq 2 to calculate σ_{kl} with cross-peak volumes from the 250 ms data set with M_0 set equal to twice the volume of the IV(1) autopeak. [b] Depth of minimum for 0.3 nm constraint in kcal/mol. [c] No cross peak seen for this proton pair; however, results from one-state model indicated that cross peak should be observed.

$\psi = -10$ to $\phi = 40, \psi = -50$. The respective conformers are shown in Figure 4, a and b. Examination of χ^2 values shows that for the HSEA conformer, χ^2 values are at least a factor of 2 larger than expectation, and as distance constraint energies are weighted more heavily a new conformation is found which fits data within experimental error for the IV–III linkage and greatly improves the fit for the II–I linkage.

One possible reason for the departure in conformation is that energy terms neglected in the HSEA calculation are important in determining the solution conformational properties of these linkages. Such terms include specific remote group effects, solvent effects, and hydrogen bonding. Examination of the potential surface as a function of the glycosidic torsional angles ϕ and ψ for both the GalNac(β1–3)Gal and Gal(β1–4)Glc linkages shows the presence of a broad single minimum, with a large portion of conformational space being within 5.0 kcal/mol of the minimum. The difference in HSEA energies between the minimum energy conformer in the presence of distance constraint pseudoenergies and the HSEA minimum energy conformer is 4.8 kcal/mol for the Gal(β1–4)Glc linkage and only 1.5 kcal/mol for the GalNac(β1–3)Gal linkage. Both of these differences are well within the range of energy terms neglected by the calculation. In the case of the Gal(β1–4)Glc linkage an additional factor, namely the neglect of the ceramide moiety, attached to the Glc residue at the anomeric carbon, must be considered as a possible source for the departure of the conformation of the Gal(β1–4)Glc linkage from the predicted conformation on the basis of the HSEA calculation alone. Bock and co-workers,[27] however, have carried out calculations on the intact glycolipid. Data from this study for the Gal(β1–4)Glc linkage are in good agreement with the data from our HSEA calculations. We must conclude that the reasons for the departure of the conformation of the Gal(β1–4)Glc linkage from the HSEA minimum lie elsewhere.

In the case of the internal Gal(α1–4)Gal (III–II) linkage, the conformational data for the linkage in the presence of distance constraint pseudoenergies are in good agreement with the HSEA minimum. Examination of the energy surface for this linkage as a function of the glycosidic torsional angles ϕ and ψ shows a smaller region of conformational space within 5.0 kcal/mol than for the other glycosidic linkage. This linkage appears more sterically crowded, and repulsive potentials are likely to dominate. For such a case, it is apparent that the HSEA calculation, alone, does an excellent job of predicting the energetics of the glycosidic linkage.

Another possible reason for the lack of agreement between the observed cross-relaxation data and the predicted cross-relaxation

(27) Bock, K.; Breimer, M. E.; Brignole, A.; Hansson, G. C.; Karlsson, K. A.; Larson, G.; Leffler, H.; Samuelsson, B. E.; Strömberg, N.; Eden, C. S.; Thurin, J. *J. Biol. Chem.* **1985**, *260*, 8545–8551.

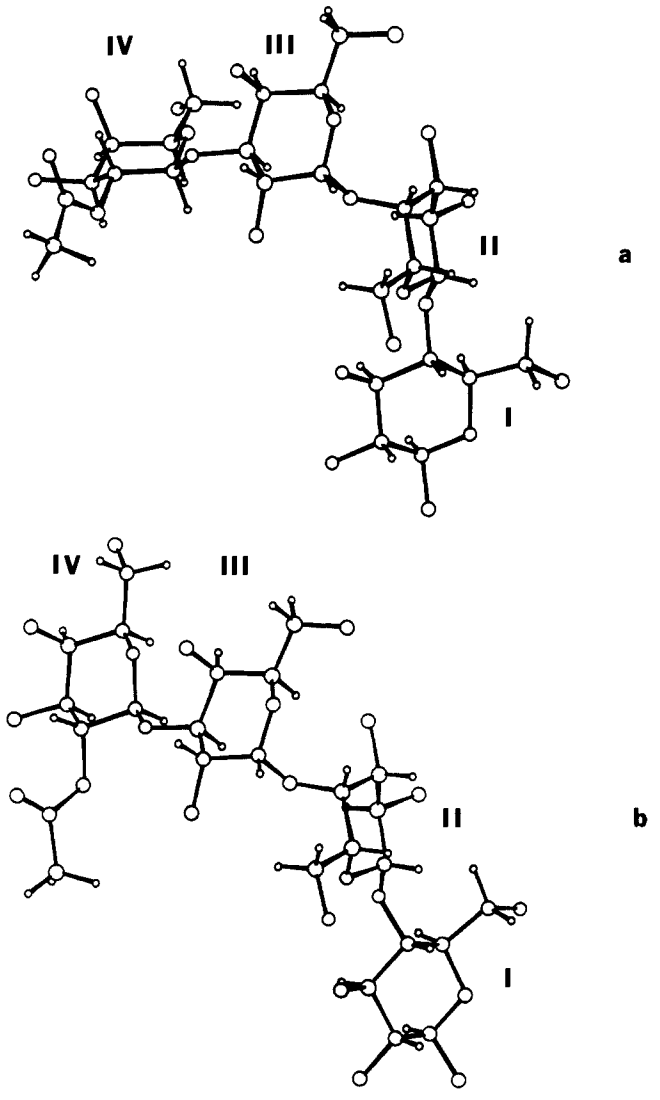

Figure 4. (a) Ball and stick drawing of the minimum energy conformation of globoside predicted on the basis of HSEA calculation alone. Hydroxyl protons are omitted since they were not considered in any of the calculations. (b) Ball and stick drawing of the minimum energy conformation of globoside predicted on the basis of combination of HSEA calculation and distance constraint pseudoenergies through the use of the one-state rigid conformer model.

rates for II–I and IV–III glycosidic bonds could be that the observed cross-relaxation data represent an average over all conformers present in solution. This possibility is a source of frequent criticism of studies which seek to treat observed cross-relaxation data as being the result of a single dominant conformer in solution. We can test this possibility through the use of our two-state model. The results of the two-state model for each linkage are also presented in Table III. For the Gal(β1–4)Glc linkage the two-state model shows only occupation of conformational states near the one-state minimum. This result, along with the lack of significant improvement in the value of χ^2 for the two-state model, increases our confidence that the one-state model is appropriate for interpreting the observed cross-relaxation data for the Gal(β1–4)Glc linkage. It should be noted that χ^2 for the Gal(β1–4)Glc linkage is significantly larger than the number of observations. This is due in large part to contribution from two factors. First, since residue I was the last residue added, there is a bias introduced into the value of χ^2 for the II–I linkage because of the very large number of long distance constraints introduced with an unrealistic 0.4-nm value. Although individually small, a significant portion of the sum of the squares of the deviations between the calculated and observed cross-relaxation rates for the II–I linkage arises from failure to fit these constraints. Second, there is a large contribution from our inability to reproduce the observed cross-relaxation rate for the II(1)–I(6a) constraint.

For the Gal(α1–4)Gal linkage, the two-state model shows occupation of conformers well displaced from one another in conformational space for all weightings of the distance constraint pseudoenergies. In each case, however, the value of χ^2 actually increases from the value predicted by the one-state model. For this linkage, we therefore also conclude that the one-state model is adequate for interpreting the observed cross-relaxation data.

In the case of the terminal GalNac(β1–3)Gal (IV–III) terminal linkage, the two-state model shows a significant occupation of conformational states well displaced from one another in conformational space as well as a small improvement in the value of χ^2 as compared to the one-state model. In the case of the two-state model χ^2 becomes slightly less than the number of non-zero weighted distance constraints, which certainly indicates that the use of a more elaborate multistate model with adjustable parameters would not be justified in fitting the data. These facts indicate that conformational averaging may be important in explaining the cross-relaxation data for the GalNac(β1–3)Gal linkage. It is possible that this linkage is conformationally flexible because of its position at the terminus of the chain.

Despite possible flexibility at the terminus, it is important to remember that the data in Table III indicate that for two of the three glycosidic linkages in globoside, the one-state model is indeed an adequate representation of the experimental cross-relaxation data. Thus we direct your attention to Figure 4b for the remainder of our discussion. We believe this to be a reasonable approximation for conformation of globoside in Me_2SO-d_6·D_2O. Despite sizable ϕ and ψ angular deviations for two of the linkages, the gross conformational properties are similar to those of the conformer, presented in Figure 4a, which is the result of the HSEA minimization, alone. The overall "L" shape is also in good agreement with the model proposed by Yu and co-workers[28] in a previous study based on model building and a less complete set of two-dimensional cross-relaxation data.

While it is interesting to speculate about the influence this particular conformation may have on receptor function, extrapolation to in vivo conditions should be done with caution because of the nonphysiological solvent used in these studies. The main value of our results is twofold: first, an illustration of a methodology for systematically integrating NMR data with energy calculations, and second, an illustration of a means for testing for conformational averaging. The methodology can easily be extended to more sophisticated molecular mechanics programs and applied in situations more closely approximating in vivo conditions.

Acknowledgment. We thank Dr. Dennis R. Hare for the use of his NMR processing software and Peter Demou for his assistance with instrumental aspects of the work. We acknowledge support of the National Institutes of Health through Grants GM33225 and NS11853 and the National Science Foundation through a predoctoral fellowship (J.N.S.). This research benefitted from instrumentation provided through the instrumentation programs of the National Institute for General Medical Sciences (GM32243S1) and the Division of Research Resources of NIH (RR02379).

Registry No. Globoside, 83333-10-2.

(28) Yu, R. K.; Koerner, T. A. W.; Demou, P. C.; Scarsdale, J. N.; Prestegard, J. H. *Adv. Exp. Med. Biol.* **1984**, *174*, 87–102.